Inorganic Chemistry

pubs.acs.org/IC

Communication

Staudinger Reactivity and Click Chemistry of Anthracene (A)-Based Azidophosphine N_3PA

André K. Eckhardt, Martin-Louis Y. Riu, Peter Müller, and Christopher C. Cummins*

Cite This: *Inorg. Chem.* 2022, 61, 1270−1274

Read Online

ACCESS | Metrics & More | Article Recommendations | Supporting Information

ABSTRACT: 11-Azido-9,10-dihydro-9,10-phosphanoanthracene (N_3**PA**) has been demonstrated recently as a transfer reagent for molecular phosphorus mononitride (PN) because it easily dissociates at room temperature into dinitrogen (N_2), PN, and anthracene (**A**). Here we report further reactivity studies of the N_3**PA** molecule including strain-promoted 1,3-dipolar cycloaddition with cyclooctyne and Staudinger-type reactivity. Calculations at the DLPNO-CCSD(T)/cc-pVTZ//PBE0-D3(BJ)/cc-pVTZ level of theory indicate that the click reaction is faster than the dissociation of N_3**PA**. The Staudinger-type reactivity enabled transfer of the NP**A** fragment to a base-stabilized silylene. The previously reported intermediate of vanadium trisanilide with an NP**A** ligand could be isolated in 61% yield and structurally characterized in a single-crystal X-ray diffraction experiment. In line with the previously reported phosphinidene reactivity of the transient vanadium phosphorus mononitride complex, thermolysis or irradiation of the complex leads to **A** elimination and formation of the corresponding vanadium PN dimer or trimer, respectively.

Inspired by Carpino's hydrazine,[1] the Cummins group developed in the past decade the synthesis of dibenzo-7λ^3-phosphanorbornadiene derivatives, which serve as molecular precursors for the release of reactive phosphorus species.[2−10] In an initial study, Velian and Cummins demonstrated the direct reaction of Mg**A**·3THF (**A** = $C_{14}H_{10}$ or anthracene; THF = tetrahydrofuran) with phosphorus dichlorides, $RPCl_2$ [R = *tert*-butyl (^{t}Bu), 2,3:5,6-dibenzo-7-azabicyclo[2.2.1]hepta-2,5-diene (dbabh), $(Me_3Si)_2N$ (HMDS), $^iPr_2N$], to afford 7λ^3-phosphanorbornadiene (RP**A**) derivatives.[2] These RP**A** compounds served as starting materials for the synthesis of further **A**-based molecular precursors for the mild release of small phosphorus-bearing species, including diphosphorus (P_2) and HCP.[3−5]

Recently, we expanded the scope of RP**A** derivatives with the synthesis and isolation of highly labile 11-azido-9,10-dihydro-9,10-phosphanoanthracene (N_3P**A**; Scheme S1).[11] N_3P**A** was shown to dissociate with a first-order kinetics half-life of roughly 30 min at room temperature to **A** and yellow-brownish polymers. Upon heating under vacuum, N_3P**A** explodes at 42 °C, and dinitrogen (N_2), phosphorus mononitride (PN), and **A** were identified as the dissociation products in a molecular-beam mass spectrometry (MS) study. In solution, PN transfer reactivity was demonstrated in the reaction of N_3P**A** with [(dppe)Fe(Cp*)(N_2)][BArF_{24}] [dppe = 1,2-bis(diphenylphosphino)ethane], leading to the formation of [(dppe)Fe(Cp*)(NP)][BArF_{24}], with the PN ligand[12] N-bonded to the iron center because of significant covalent iron−pnictogen bond character and associated less unfavorable Pauli repulsion in the metal−ligand interaction. Here we demonstrate further reactivity studies of N_3P**A** with cyclooctyne, a base-stabilized silylene, and reinvestigate the proposed reaction mechanism in the synthesis of a transient vanadium PN complex, PNV(N[^{t}Bu]Ar)$_3$ (Ar = 3,5-$Me_2C_6H_3$).

PN-trapping experiments with N_3P**A** were conducted in neat cyclohexadiene and 2,3-dimethyl-1,3-butadiene, respectively. However, stirring the reaction mixture at room temperature or at 60 °C resulted in rapid PN polymerization, as indicated by the precipitation of orange-brown polymers and no resonances in the ^{31}P NMR spectrum. The experiment was repeated and the solution irradiated in a quartz NMR tube with λ = 254 nm light for 10 min at room temperature, but the result was the same. Note that rapid polymerization is also reported for gaseous PN, which produces white powder coatings on surfaces and limits high PN concentrations for spectroscopic measurements.[13] The color of the PN polymers is reported to change depending on the nitrogen content.[14,15] In stark contrast to P_2, PN presumably does not show any triple-bond reactivity with dienes under similar mild reaction conditions because of rapid polymerization.[16,17] Further PN-trapping experiments with 3,5-diphenyl-2-phosphafuran,[18] different azide sources, or alkynes were also not successful. We calculated the reaction barriers for the [4 + 2] cycloaddition reactions of 1,3-butadiene with P_2 (Figure 1, top) and PN (Figure 1, bottom), respectively, at the DLPNO-CCSD(T)/cc-pVTZ//B3LYP-D3(BJ)/cc-pVTZ + thermal correction to Gibbs free energy at 298.15 K level of theory. The cycloaddition reaction of 1,3-butadiene with P_2 is highly symmetric and associated with a reaction barrier of 15.3 kcal mol^{-1} at room temperature (Figure 1, top). The low reaction barrier is in good agreement with that in the previous P_2-

Received: December 2, 2021
Published: January 12, 2022

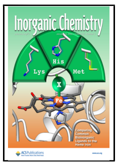

https://doi.org/10.1021/acs.inorgchem.1c03753

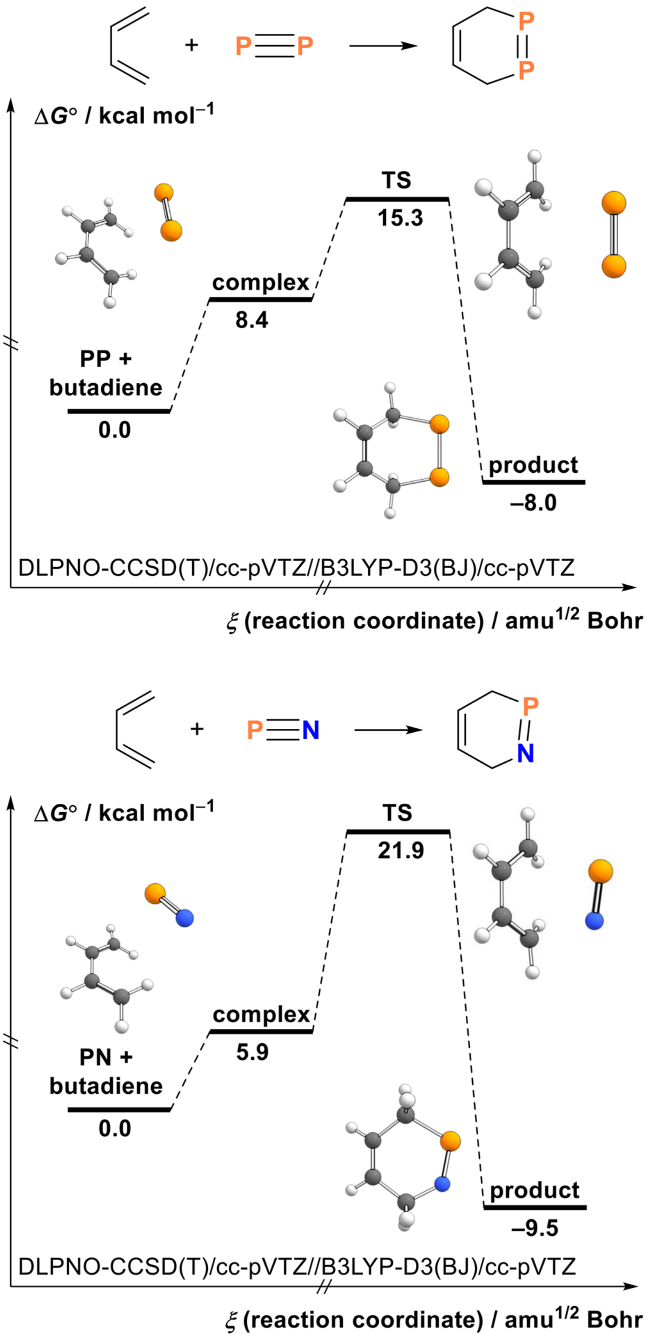

Figure 1. Computed reaction barriers for the [4 + 2] cycloaddition reactions of 1,3-butadiene with P_2 (top) and PN (bottom), respectively. The Gibbs free energy values are computed for T = 298.15 K. Color code: carbon = gray; hydrogen = white; nitrogen = blue; phosphorus = orange.

trapping experiments.[16,17] Because of the different atomic and orbital sizes of phosphorus versus nitrogen, the cycloaddition of 1,3-butadiene and PN is more asymmetric and the computed reaction barrier is increased by 6.6 kcal mol^{-1} to 21.9 kcal mol^{-1}. Note that the energy for *trans*−*cis* interconversion of 1,3-butadiene is not included here.[19] According to our experimental results, it seems likely that the barrier for PN polymerization is much lower in energy.

The addition of cyclooctyne to a stirring solution of N_3**PA** in THF at room temperature did not lead to color changes or the formation of any precipitate. ^{31}P NMR analysis of the reaction mixture revealed a new triplet resonance at δ 154 ppm with a coupling constant of $^3J_{HP}$ = 13.3 Hz, indicating that the product formed in this reaction contains a phosphorus center bound to **A**. A diethyl ether solution of the crude reaction mixture was filtered through a plug of Celite and charcoal to remove free **A**, and the filtrate was cooled to −20 °C to crystallize out the product. Single-crystal X-ray diffraction confirmed triazole **1** as the 1,3-dipolar cycloaddition product (click product) between the azide unit of N_3**PA** and cyclooctyne (Figure 2). The computed low reaction barrier of the strain-promoted [3 + 2] cycloaddition of phenyl azide and cyclooctyne is consistent with our experimental findings.[20] The strain-promoted click reaction is faster than the decay of N_3**PA**.[21] After **1** was stirred in THF at room temperature for 2 h, a small triplet signal at δ 165 ppm appeared in the ^{31}P NMR spectrum. Complete conversion of compound **1** to the species corresponding to the new resonance was achieved by heating the solution for 3 h at 80 °C. Crystals of the product were grown from diethyl ether and characterized by single-crystal X-ray crystallography, revealing a [1,2] shift of the **PA** unit to the central nitrogen atom in the triazole ring and the formation of **2** (Figure 2). Surprisingly, we could find no literature precedent for phosphorus-substituted triazoles, and only related isomeric triazaphospholes are well-studied.[22] Heating of **2** in toluene at 120 °C for 2 h led to the release of **A** and no resonances in the ^{31}P NMR spectrum. Phosphinidene-trapping experiments with an excess of cyclohexene were not successful.

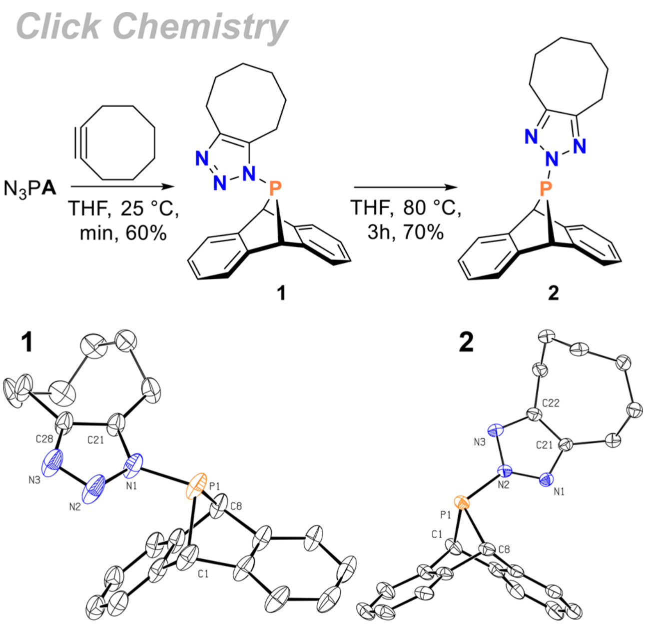

Figure 2. Top: Strain-promoted click chemistry of N_3**PA** and cyclooctyne. Bottom: Molecular structures of **1** and **2**, with thermal ellipsoids shown at the 50% probability level. Hydrogen atoms are omitted for the sake of clarity. Selected interatomic distances (Å) for **1**: P1−N1, 1.7670(14); P1−C1, 1.886(2); P1−C8, 1.8956(18); N1−C21, 1.3549(19); N1−N2, 1.368(2); N2−N3, 1.312(2); C21−C28, 1.379(2). Selected interatomic distances (Å) for **2**: P1−N2, 1.7564(13); P1−C1, 1.8921(17); P1−C8, 1.9028(17); N1−N2, 1.329(4); N1−C21, 1.324(8); C21−C22, 1.401(9).

We explored the potential energy surface around N_3**PA** and cyclooctyne at the DLPNO-CCSD(T)/cc-pVTZ//PBE0-D3(BJ)/cc-pVTZ + thermal correction to Gibbs free energy at 298.15 K level of theory (Figure 3). We located a transition state (**TS1**) that is 20.9 kcal mol^{-1} higher in energy than those of the two reactants. This barrier is lower in energy (2.4 kcal mol^{-1}) than the previously computed decomposition barrier of N_3**PA** (23.3 kcal mol^{-1}) at the same level of theory. Taking the experimentally determined dissociation barrier for N_3**PA** of $\Delta G^{\ddagger} = 22.1 \pm 1.5$ kcal mol^{-1} at 298 K into account, we assume that the computed barriers are in general slightly higher in energy than the experimental ones. Consistent with the high strain energy of cyclooctyne, the reaction is highly exothermic (−58.3 kcal mol^{-1}). A second transition state (**TS2**) that describes the experimentally observed rearrangement is associated with a 26.3 kcal mol^{-1} high reaction barrier. The rearrangement is slightly exothermic by 4.8 kcal mol^{-1}. Note that the computed minimum structure for **2** differs from the geometry of the crystalline compound. The triazole ring is rotated by almost 90° around the central P−N bond and is now almost in a position parallel to the **A** unit.

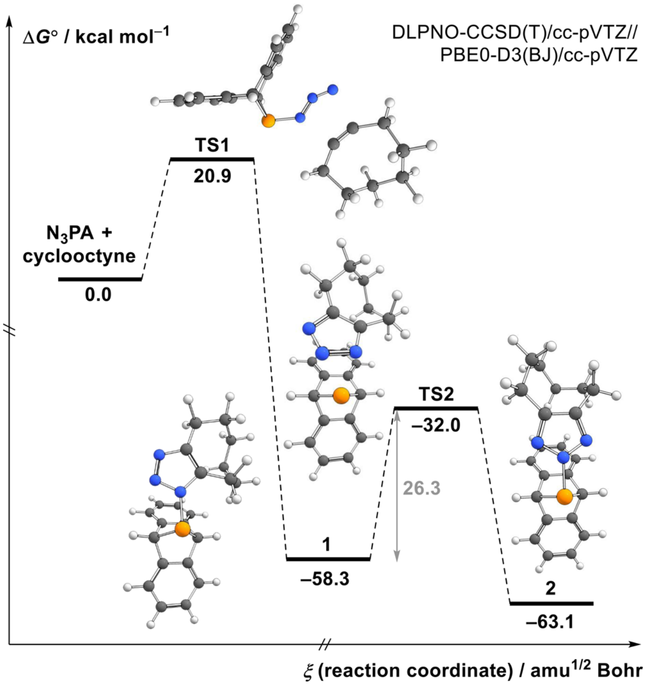

Figure 3. Computed minimum energy pathway for the reaction of N_3**PA** with cyclooctyne. The Gibbs free energy values were computed for T = 298.15 K.

Inspired by the work of Bertrand and co-workers, who demonstrated the stabilization of PN by N-heterocyclic carbenes (NHCs), we investigated the reaction of N_3**PA** with an NHC.[23] The addition of N_3**PA** to a thawing solution of 2 equiv of 1,3-bis(2,6-diisopropylphenyl)imidazol-2-ylidene (Ipr)[24] resulted in gas evolution during warming and a color change to orange. After the solution was stirred for 1 h, we analyzed the crude reaction mixture by $^{31}P\{^{1}H\}$ and ^{31}P NMR spectroscopy and observed a new resonance at δ 285.5 ppm; note that the NHC-PN adduct by Bertrand and co-workers was reported at δ 134.0 ppm.[23] However, we were not able to isolate any reaction product. Therefore, we repeated the reaction in a similar fashion with a base-stabilized silylene (**3**; Figure 4).[25] The thawing yellow solution rapidly became blue, followed by orange, and finally slightly yellow after stirring for 30 min during warming. In addition, gas evolution was observed. The ^{31}P NMR spectrum of the crude reaction mixture exhibited a single triplet resonance at δ 154 ppm with a coupling constant of $^{3}J_{HP}$ = 13.7 Hz, indicating a clean chemical transformation with the **A** unit still attached to phosphorus. Single-crystal X-ray diffraction crystallography on a crystal grown from a pentane solution revealed that a Staudinger-type reaction[26] had ensued between N_3**PA** and the silylene, leading to the formation of **APN** adduct **4**, with concomitant release of N_2 (Figure 4). The adduct **4** easily eliminated **A** when heated; however, no resonances were observed in the ^{31}P NMR spectrum. Additionally, the compound was highly moisture-sensitive, as was accidentally found by X-ray crystallography and AccuTOF-DART MS studies. Upon the addition of water, compound **4** almost completely hydrolyzed within seconds and ring-opened to compound **5**. Note that there was an intramolecular hydrogen bond between the silanol and the nearby imine function (Figure 4). In contrast to Ipr, **3** was able to stabilize the Staudinger reaction product.

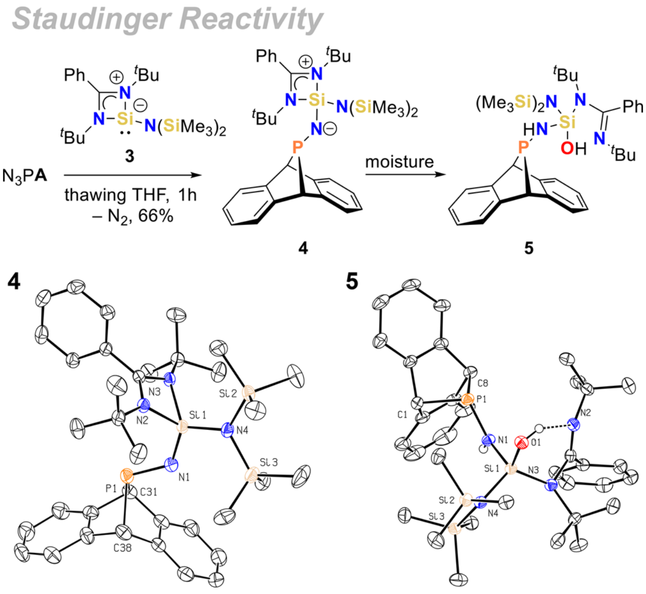

Figure 4. Top: Staudinger-type reactivity of N_3**PA** and base-stabilized silylene **3** followed by hydrolysis. Bottom: Molecular structures of **4** and **5**, with thermal ellipsoids shown at the 50% probability level. Hydrogen atoms are omitted for the sake of clarity. Selected interatomic distances (Å) for **4**: P1−N1, 1.6320(11); P1−C31, 1.937(3); P1−C38, 1.938(3); N1−Si1, 1.6289(12). Selected interatomic distances (Å) for **5**: P1−N1, 1.6862(18); P1−C1, 1.912(2); P1−C8, 1.926(2); N1−Si1, 1.7425(18).

The observed Staudinger-type reactivity (*vide supra*) motivated us to revisit the proposed reaction mechanism in formation of the transient vanadium PN complex, (PN)V(N[^{t}Bu]Ar)$_3$.[27] In the reaction of Na[NV(N[^{t}Bu]Ar)$_3$] with ClPA, only trimeric [(PN)V(N[^{t}Bu]Ar)$_3$]$_3$ (**7**), which forms dimeric [(PN)V(N[^{t}Bu]Ar)$_3$]$_2$ (**8**) upon heating, could be isolated. **A**-bound (APN)V(N[^{t}Bu]Ar)$_3$ (**6**) and free (PN)V(N[^{t}Bu]Ar)$_3$ were proposed as reactive intermediates in this transformation. However, even in a low-temperature NMR experiment between −60 and +23 °C, neither of the intermediates were detected. Hence, the two complexes were assumed to be thermally unstable. The careful addition of solid N_3**PA** to a dark-green stirring solution of V(N[^{t}Bu]Ar)$_3$ in diethyl ether at room temperature led to an immediate color change to dark red and gas evolution. The crude $^{31}P\{^{1}H\}$ and

^{51}V NMR spectra showed broad signals at δ 249 and δ 27 ppm, respectively. In addition, a doublet at δ 4.95 ppm was observed in the ^{1}H NMR spectrum, indicative of bridgehead protons of **6**. After workup, bright-red solids were isolated in 61% yield. A representative sample was crystallized from cold (−20 °C) diethyl ether over 2 days, yielding dark-red crystals that were analyzed in an X-ray crystallographic study. This experiment confirmed the formation of **6** (Figure 5). Heating of the complex in benzene at 80 °C resulted in the formation of dimer **8** via trimeric **7**, as followed by ^{51}V NMR spectroscopy (Figure S19). Irradiation of **6** at room temperature with λ = 254 nm light also released **A**, and trimeric **7** was formed (Figure 5).

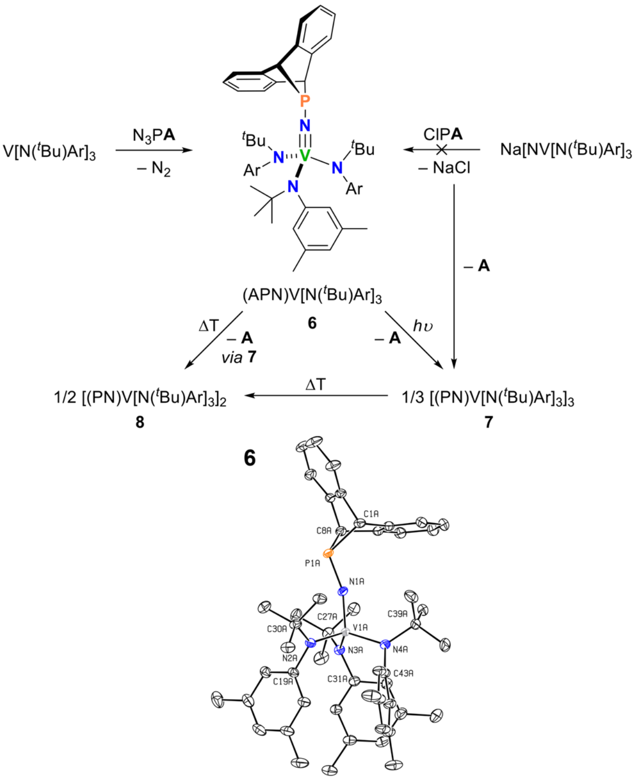

Figure 5. Top: Synthesis of **6** and subsequent thermally and photochemically induced oligomerization reactions. Bottom: Molecular structure of **6**, with thermal ellipsoids shown at the 50% probability level. Hydrogen atoms are omitted for the sake of clarity. Selected interatomic distances (Å): P1A−N1A, 1.699(1); P1A−C1A, 1.910(1); P1A−C8A, 1.904(1); N1A−V1A, 1.693(8). Selected interatomic bond angles (deg): C1A−P1A−C8A, 79.3(5); P1A−N1A−V1A, 146.8(1).

The niobaziridine−hydride complex Nb(H)(η^2-^{t}Bu(H)-CNAr)(N[Np]Ar)$_2$ (Np = neopentyl; Ar = 3,5-$C_6H_3Me_2$) was reported to react with elemental phosphorus (P_4) to yield the bridging diphosphide complex (μ_2:η^2,η^2-P_2)[Nb(N[Np]-Ar)$_3$]$_2$.[28] Treatment of the niobaziridine−hydride complex with N_3**PA** resulted in a reactivity similar to that with the vanadium trisanilide complex (*vide supra*) and formation of the (**APN**)Nb(N[^{t}Bu]Ar)$_3$ complex (**9**; see Figure S20 for further synthetic details). The heating or treatment of this complex with another equivalent of the niobaziridine−hydride complex did not result in formation of the bridging phosphorus mononitride complex. Besides free **A** resonances in the ^{1}H NMR spectrum, we only observed a single resonance in the ^{31}P NMR at δ 115 ppm, which is tentatively assigned to an oligomerized niobium−PN complex based on free **A** resonances and our findings of the related vanadium system (Figures S17 and S18).

Caution! *The handling of azide compounds should be done with the necessary safety precautions.*[29] *No direct explosions of N_3PA were encountered when it was diluted in organic solvents or carefully dried under vacuum below room temperature. The treatment of transition-metal complexes in solution with solid N_3PA can cause a spontaneous explosive decomposition of N_3PA and should be avoided or solid N_3PA should only be added in portions of a few milligrams, respectively.*

■ ASSOCIATED CONTENT

Supporting Information

The Supporting Information is available free of charge at https://pubs.acs.org/doi/10.1021/acs.inorgchem.1c03753.

> Full synthetic and computational details, including preparative procedures and spectroscopic data for characterization of the compounds (PDF)

Accession Codes

CCDC 2110926−2110930 and 2120073 contain the supplementary crystallographic data for this paper. These data can be obtained free of charge via www.ccdc.cam.ac.uk/data_request/cif, or by emailing data_request@ccdc.cam.ac.uk, or by contacting The Cambridge Crystallographic Data Centre, 12 Union Road, Cambridge CB2 1EZ, UK; fax: +44 1223 336033.

■ AUTHOR INFORMATION

Corresponding Author

Christopher C. Cummins − *Department of Chemistry, Massachusetts Institute of Technology, Cambridge, Massachusetts 02139, United States;* orcid.org/0000-0003-2568-3269; Email: ccummins@mit.edu

Authors

André K. Eckhardt − *Department of Chemistry, Massachusetts Institute of Technology, Cambridge, Massachusetts 02139, United States;* orcid.org/0000-0003-1029-9272

Martin-Louis Y. Riu − *Department of Chemistry, Massachusetts Institute of Technology, Cambridge, Massachusetts 02139, United States;* orcid.org/0000-0002-0900-3545

Peter Müller − *Department of Chemistry, Massachusetts Institute of Technology, Cambridge, Massachusetts 02139, United States;* orcid.org/0000-0001-6530-3852

Complete contact information is available at: https://pubs.acs.org/10.1021/acs.inorgchem.1c03753

Notes

The authors declare no competing financial interest.

■ ACKNOWLEDGMENTS

A.K.E. thanks the Alexander von Humboldt Foundation for a Feodor Lynen postdoctoral fellowship. P.M. thanks Bruce Noll for helpful discussions. The authors thank Marc-André Courtemanche for his careful proofreading and suggestions. This material is based on research supported by the National Science Foundation under Grant CHE-1955612. We thank all MIT DCIF staff members for technical support.

■ REFERENCES

(1) Carpino, L. A.; Padykula, R. E.; Barr, D. E.; Hall, F. H.; Krause, J. G.; Dufresne, R. F.; Thoman, C. J. Synthesis, characterization, and thermolysis of 7-amino-7-azabenzonorbornadienes. *J. Org. Chem.* **1988**, *53*, 2565−2572.

(2) Velian, A.; Cummins, C. C. Facile Synthesis of Dibenzo-7λ^3-phosphanorbornadiene Derivatives Using Magnesium Anthracene. *J. Am. Chem. Soc.* **2012**, *134*, 13978−13981.

(3) Velian, A.; Nava, M.; Temprado, M.; Zhou, Y.; Field, R. W.; Cummins, C. C. A Retro Diels−Alder Route to Diphosphorus Chemistry: Molecular Precursor Synthesis, Kinetics of P_2 Transfer to 1,3-Dienes, and Detection of P_2 by Molecular Beam Mass Spectrometry. *J. Am. Chem. Soc.* **2014**, *136*, 13586−13589.

(4) Velian, A.; Cummins, C. C. Synthesis and characterization of $P_2N_3^-$: An aromatic ion composed of phosphorus and nitrogen. *Science* **2015**, *348*, 1001.

(5) Transue, W. J.; Velian, A.; Nava, M.; Martin-Drumel, M.-A.; Womack, C. C.; Jiang, J.; Hou, G.-L.; Wang, X.-B.; McCarthy, M. C.; Field, R. W.; Cummins, C. C. A Molecular Precursor to Phosphaethyne and Its Application in Synthesis of the Aromatic 1,2,3,4-Phosphatriazolate Anion. *J. Am. Chem. Soc.* **2016**, *138*, 6731−6734.

(6) Transue, W. J.; Velian, A.; Nava, M.; García-Iriepa, C.; Temprado, M.; Cummins, C. C. Mechanism and Scope of Phosphinidene Transfer from Dibenzo-7-phosphanorbornadiene Compounds. *J. Am. Chem. Soc.* **2017**, *139*, 10822−10831.

(7) Transue, W. J.; Yang, J.; Nava, M.; Sergeyev, I. V.; Barnum, T. J.; McCarthy, M. C.; Cummins, C. C. Synthetic and Spectroscopic Investigations Enabled by Modular Synthesis of Molecular Phosphaalkyne Precursors. *J. Am. Chem. Soc.* **2018**, *140*, 17985−17991.

(8) Transue, W. J.; Nava, M.; Terban, M. W.; Yang, J.; Greenberg, M. W.; Wu, G.; Foreman, E. S.; Mustoe, C. L.; Kennepohl, P.; Owen, J. S.; Billinge, S. J. L.; Kulik, H. J.; Cummins, C. C. Anthracene as a Launchpad for a Phosphinidene Sulfide and for Generation of a Phosphorus−Sulfur Material Having the Composition P_2S, a Vulcanized Red Phosphorus That Is Yellow. *J. Am. Chem. Soc.* **2019**, *141*, 431−440.

(9) Riu, M. Y.; Transue, W. J.; Rall, J. M.; Cummins, C. C. An Azophosphine Synthetic Equivalent of Mesitylphosphaazide and Its 1,3-Dipolar Cycloaddition Reactions. *J. Am. Chem. Soc.* **2021**, *143*, 7635−7640.

(10) Eckhardt, A. K.; Riu, M. Y.; Müller, P.; Cummins, C. C. Frustrated Lewis Pair Stabilized Phosphoryl Nitride (NPO), a Monophosphorus Analogue of Nitrous Oxide (N_2O). *J. Am. Chem. Soc.* **2021**, *143*, 21252−21257.

(11) Eckhardt, A. K.; Riu, M.-L. Y.; Ye, M.; Müller, P.; Bistoni, G.; Cummins, C. C., Taming Phosphorus Mononitride (PN). 2021-08-26 Version 1. *ChemRxiV (Inorganic Chemistry)*. **2021** DOI: 10.33774/chemrxiv-2021-zxtmf (accessed 08-26-2021).

(12) Martinez, J. L.; Lutz, S. A.; Beagan, D. M.; Gao, X.; Pink, M.; Chen, C.-H.; Carta, V.; Moënne-Loccoz, P.; Smith, J. M. Stabilization of the Dinitrogen Analogue, Phosphorus Nitride. *ACS Cent. Sci.* **2020**, *6*, 1572−1577.

(13) Ahmad, I. K.; Hamilton, P. A. The Fourier Transform Infrared Spectrum of PN. *J. Mol. Spectrosc.* **1995**, *169*, 286−291.

(14) Moldenhauer, W.; Dörsam, H. Über die Vereinigung von Phosphor und Stickstoff unter dem Einflusse elektrischer Entladungen. *Ber. dtsch. Chem. Ges. A/B* **1926**, *59*, 926−931.

(15) Holleman, A. F. *Lehrbuch der anorganischen Chemie*; Walter de Gruyter GmbH & Co. KG, 2019.

(16) Piro, N. A.; Figueroa, J. S.; McKellar, J. T.; Cummins, C. C. Triple-Bond Reactivity of Diphosphorus Molecules. *Science* **2006**, *313*, 1276.

(17) Hering, C.; Schulz, A.; Villinger, A. Diatomic PN − trapped in a cyclo-tetraphosphazene. *Chem. Sci.* **2014**, *5*, 1064−1073.

(18) Riu, M.-L. Y.; Cummins, C. C. 3,5-Diphenyl-2-phosphafuran: Synthesis, Structure, and Thermally Reversible [4 + 2] Cycloaddition Chemistry. *J. Org. Chem.* **2020**, *85*, 14810−14816.

(19) Baraban, J. H.; Martin-Drumel, M.-A.; Changala, P. B.; Eibenberger, S.; Nava, M.; Patterson, D.; Stanton, J. F.; Ellison, G. B.; McCarthy, M. C. The Molecular Structure of gauche-1,3-Butadiene: Experimental Establishment of Non-planarity. *Angew. Chem., Int. Ed.* **2018**, *57*, 1821−1825.

(20) Breugst, M.; Reissig, H.-U. The Huisgen Reaction: Milestones of the 1,3-Dipolar Cycloaddition. *Angew. Chem., Int. Ed.* **2020**, *59*, 12293−12307.

(21) Ess, D. H.; Jones, G. O.; Houk, K. N. Transition States of Strain-Promoted Metal-Free Click Chemistry: 1,3-Dipolar Cycloadditions of Phenyl Azide and Cyclooctynes. *Org. Lett.* **2008**, *10*, 1633−1636.

(22) Sklorz, J. A. W.; Müller, C. Recent Developments in the Chemistry of 3H-1,2,3,4-Triazaphosphole Derivatives. *Eur. J. Inorg. Chem.* **2016**, *2016*, 595−606.

(23) Kinjo, R.; Donnadieu, B.; Bertrand, G. Isolation of a Carbene-Stabilized Phosphorus Mononitride and Its Radical Cation (PN+.). *Angew. Chem., Int. Ed.* **2010**, *49*, 5930−5933.

(24) Huang, J.; Nolan, S. P. Efficient Cross-Coupling of Aryl Chlorides with Aryl Grignard Reagents (Kumada Reaction) Mediated by a Palladium/Imidazolium Chloride System. *J. Am. Chem. Soc.* **1999**, *121*, 9889−9890.

(25) Sen, S. S.; Hey, J.; Herbst-Irmer, R.; Roesky, H. W.; Stalke, D. Striking Stability of a Substituted Silicon(II) Bis(trimethylsilyl)amide and the Facile Si−Me Bond Cleavage without a Transition Metal Catalyst. *J. Am. Chem. Soc.* **2011**, *133*, 12311−12316.

(26) Staudinger, H.; Meyer, J. Über neue organische Phosphorverbindungen III. Phosphinmethylenderivate und Phosphinimine. *Helv. Chim. Acta* **1919**, *2*, 635−646.

(27) Courtemanche, M.-A.; Transue, W. J.; Cummins, C. C. Phosphinidene Reactivity of a Transient Vanadium P≡N Complex. *J. Am. Chem. Soc.* **2016**, *138*, 16220−16223.

(28) Figueroa, J. S.; Cummins, C. C. The Niobaziridine−Hydride Functional Group: Synthesis and Divergent Reactivity. *J. Am. Chem. Soc.* **2003**, *125*, 4020−4021.

(29) *Information on Azide Compounds*; Stanford Environmental Health & Safety, https://ehs.stanford.edu/reference/information-azide-compounds (accessed 08-24-2021).